High-performance E-band continuous transverse stub array antenna with a 45° linear polarizer

You, Yang; Lu, Yunlong; Wang, Yi; Yang, Wen-wen; Hao, Zhang-cheng; You, Qingchun; Huang, Jifu

DOI:
10.1109/LAWP.2019.2940127

High-Performance E-Band Continuous Transverse Stub Array Antenna with a 45° Linear Polarizer

Yang You, Yunlong Lu, Yi Wang, *Senior Member, IEEE*, Wen-Wen Yang, *Member, IEEE*, Zhang-Cheng Hao, *Senior Member, IEEE*, Qingchun You, and Jifu Huang

***Abstract*—This letter presents a continuous transverse stub (CTS) array antenna with high aperture efficiency, low sidelobes and cross-polarization characteristics over E-band. The antenna consists of a full-corporate feed 32-slot CTS array and a 45° linear polarizer. A multiple-aperture excited parallel-plate waveguide structure works as a linear source generator to generate the quasi-TEM wave with a uniform amplitude distribution over the whole operating band from 71 to 86 GHz. The 45° linear polarizer contains two layers of slots, shifting the linear polarization from the principal E-plane (ϕ=90°) to the intended E-plane (ϕ=135°). The array antenna achieves the low cross-polarization and side-lobe level (SLL) while maintaining high aperture efficiency. Measurement results show that the antenna has an aperture efficiency of over 74% with the peak gains of better than 37.9 dBi over the whole E-band, while the far-field SLLs in the intended E- and H-planes approach the ETSI class-IV envelope standard.**

Index Terms— ***Continuous transverse stub array, low sidelobe levels, 45° linear polarizer.***

I. Introduction

Millimeter-wave (mmW) E-band (71–76 and 81–86 GHz) has been allocated for multi-Gbps point-to-point wireless links [1], [2]. Wideband, high-gain planar array antenna with lower SLLs and cross-polarization are highly desired in fixed radio links, as specified by ETSI or FCC. The slotted waveguide (SW) array antennas have been a top choice for high performance mmW antennas [3]. But it commonly suffers from a narrow bandwidth [4].

Recently, continuous transverse stub (CTS) array antennas have been considered a competitive technology for wideband and high-gain antenna systems [5]-[10]. Compared with conventional SW antennas, the radiation slot in a CTS antenna has a larger aperture size and supports quasi-TEM mode. These lead to a higher aperture efficiency and wider operating band. There have been some recently reported work [8-10]. Unfortunately, all suffer from relative high side lobe levels (SLLs). In [11], an E-band low SLL CTS array based on amplitude tapering excitation was reported. However, amplitude tapering, as a common method to suppress sidelobes, generally reduces the antenna aperture efficiency due to the gradient amplitude excitation [12], [13]. One alternative approach to achieve low SLLs without sacrificing aperture efficiency is to take advantage of the low sidelobe characteristics in the non-principal planes [14-16]. The key of this approach is to shift the linear polarization to the desired low SLL plane. All the work in [14-16] was based on SW structures, and it remains a challenge to have a high aperture efficiency CTS array antenna with low SLLs and cross-polarization at the same time.

This letter aims to design a high-performance E-band CTS array antenna to tackle this challenge. The demonstrated antenna is well suited for current and emerging mmW applications such as 5G and point-to-point communication links.

II. Antenna Configuration and Analysis

Fig. 1(a) shows the configuration of the proposed array antenna. It consists of two parts: one is the uniformly excited full-corporate feed 32-slot CTS array, different from the tapered excitation in [11], and the other is the 45° linear polarizer. The CTS array contains three metal layers. They are radiation layer in M2, cavity layer in M3 and feed network in M4. The feed network is a 256-way (16×16) T-junction power divider with a standard input waveguide at the center on the back side. The cavity layer contains 256 (16×16) 1-to-4 vertical power dividers. Each output signal from the feed network is fed to the 1-to-4 divider into four paths to support two radiation slots in the radiation layer. There are 32 radiation slots in total in M2 to realize a high gain. The 45° linear polarizer in M1 is on top of the CTS array and used to shift the principal E- and H-planes to the diagonal directions in order to suppress the sidelobes in the intended E- and H-planes. Fig. 1(b) illustrates the definitions of the principal E- (ϕ=90°) and H- (ϕ=0°) planes and the intended E- (ϕ=135°) and H- (ϕ=45°) planes. With the polarizer, the linear polarizations of the CTS array are in the intended E-planes. Otherwise, the polarizations are in the principal planes.

This work was supported partly by National Natural Science Foundation of China under Projects 61801252, 61631012 and U1809203, in part by Opening Project of State Key Laboratory of High Performance Ceramics and Superfine Microstructure under Project SKL201708SIC and K.C. Wong Magna Fund in Ningbo University. (*Corresponding author: Yunlong Lu.*)

Y. You, Q. You and J. Huang are with the Faculty of Electrical Engineering and Computer Science, Ningbo University, Ningbo, Zhejiang, 315211, China.

Y. Lu is with the Faculty of Electrical Engineering and Computer Science, Ningbo University, Ningbo 315211, China, and also with the State Key Laboratory of High Performance Ceramics and Superfine Microstructure, Shanghai 200050, China. (e-mail: luyunlong@nbu.edu.cn).

Y. Wang is with School of Engineering, University of Birmingham, B15 2TT, United Kingdom (e-mail: y.wang.1@bham.ac.uk).

W. Yang is with School of Information Science and Technology, Nantong University, Nantong 226019, China

Z. Hao is with State Key Laboratory of Millimeter Waves, Southeast University, Nanjing 210096, China

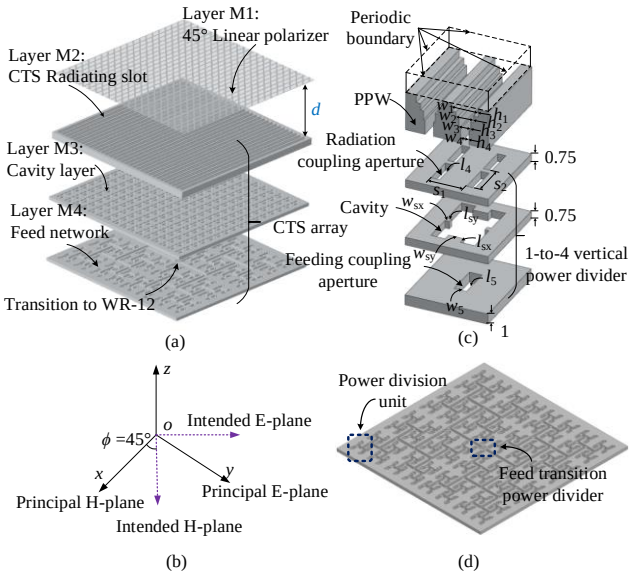

Fig. 1. Configuration of the proposed array antenna: (a) 3-D overview; (b) Definition of E- and H-planes; (c) Subarray of the CST array; (d) Feed network. All dimensions are given in millimeters.

Conveniently, the 32-slot CTS array contained within M2 and M3 can be decomposed into subarrays by setting periodic boundary conditions. Each subarray corresponds to one output port of the feed network in M4. More design details are given as follows.

A. Subarray

The subarray is shown in Fig. 1(c). It consists of two radiating slot elements and a 1-to-4 vertical power divider, without the 45° linear polarizer. The radiation slot has a stepped and flared impedance transformer to match the parallel-plate waveguide (PPW) to free space. The 1-to-4 divider contains a coupling aperture on the feed side, a cavity-backed and four radiation coupling apertures. The distances (s_1 and s_2) between the radiation coupling apertures in the *x*- and *y*-directions are both less than one free-space wavelength of the highest operating frequency to minimize the grating lobes. The perturbation stubs with dimensions of w_{sx} and l_{sy} in the *y*-direction are employed to improve the output amplitude and phase balances, whereas the other perturbation stubs with dimensions of w_{sy} and l_{sx} in the *x*-direction are to achieve a good impedance matching [17]. The optimized parameters are as follows (unit: mm): s_1=3.4, s_2=3.4, w_{sx}=0.4, l_{sy}=0.5, w_{sy}=1.46, l_{sx}=0.7, w_1=2.52, h_1=0.74, w_2=1.66, h_2=0.66, w_3=1.12, h_3=0.92, w_4=0.8, h_4=1.4, l_4=2.9, w_5=1.2, l_5=3.2.

The long radiation slots in the CTS array are excited by quasi-TEM waves. This is achieved by combining the multiple radiation coupling aperture of the subarrays and exciting the PPW structure, which works as the linear source generator (LSG), as shown in Fig. 1. Each row of coupling apertures in the *x*-direction convert the TE_{10} mode to a quasi-TEM wave in the PPW. To maximize aperture efficiency, the amplitude of the quasi-TEM wave along the PPW has been optimized to be as uniform as possible. This has been discussed in detail in our previous work [9].

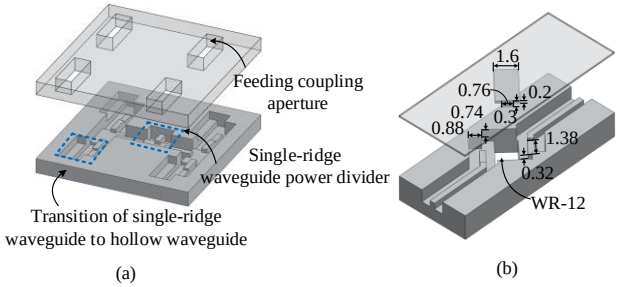

Fig. 2 Configuration of the feed network. (a) H-shape power division unit, (b) Transition power divider. All dimensions are given in millimeters.

B. Feed Network

To support the 16×16 sub-arrays, a 1-to-256 power divider is designed based on 64 (8×8) equal spilt power division units in layer M4, as shown in Fig. 1 (d). Each unit is an H-shape 1-to-4 single-ridge waveguide power divider. It consists of three H-plane T-junction dividers. Fig. 2(a) shows the configuration of the H-shape power division unit and feed transition power divider. At each output port of the feeding network, there is a transition structure from single-ridge waveguide to hollow waveguide. The input port of the array is a standard WR-12 waveguide at the center of feed network. This is followed by a two-way power divider with single-ridge waveguide outputs. A transition power divider (shown in Fig. 2(b)) is used to rotate the standard WR-12 rectangular waveguide opening to parallel to the slots on the top layer of the polarizer. This facilitates connections to the measurement equipment.

C. 45° Linear Polarizer

The 45° linear polarizer is utilized to shift the linear polarization to the desired low SLL plane, which decreases the radiation pattern envelope. The structure is inset in Fig. 3(a). It consists of two layers of slots on a 0.25 mm substrate of polycarbonate with ε_r = 3.0. The slots in the bottom layer is oriented in the *x*-direction, matching the direction of the radiation slots as shown in Fig. 1(a), and the other in 45°. The incident plane wave polarized in the *y*-direction from the long radiating slots passes the bottom grids but emerges from the top grid layer with a 45° polarization rotation.

The adverse influence of the polarizer on the antenna performance should be minimized. This is guaranteed by the slot period p_6 of the polarizer (with the width of metal strip w_6 fixed at 0.15 mm) and the distance *d* (labeled in Fig. 1(a)) between the polarizer and CTS slot. To minimize the reflection from the 45° polarizer, *d* should be about a quarter-wavelength, which is set to be 1.2 mm in this design. The parameter p_6 is chosen to maximize the transmission of perpendicular field component and reflection of the parallel field components [18]. To save computational time without losing generality, the 45° linear polarizer is simulated with a small array of 2×2-subarrays using the optimized parameters given in Section II-A. Fig. 3(a) shows a parameter study of the polarizer as a function of p_6. It can be seen that the optimal value of p_6 should be 0.43 mm, as the peak gain reaches the maximum.

The effect of the 45° linear polarizer on the antenna performance is investigated. Fig. 3(b) shows the comparison of reflection coefficients and peak gains with and without the

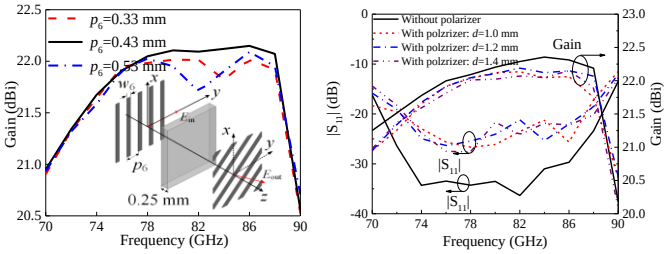

(a) (b)

Fig. 3 Analysis of the 45° linear polarizer. (a) Simulated peak gain with different periods p_6; (b) Simulated peak gain and $|S_{11}|$ with and without the polarizer.

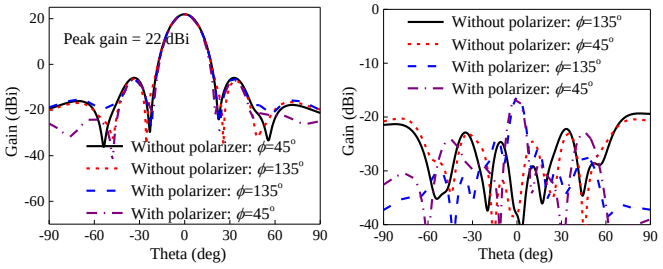

(a) (b)

Fig. 4 Radiation patterns at 78.5 GHz with and without the polarizer: (a) Co-pol, (b) Cross-pol.

polarizer. With the optimized polarizer, a good impedance matching of $|S_{11}|$<-20 dB is achieved over the desired frequency range. The peak gain with the polarizer drops by less than 0.3 dB mainly due to its insertion loss. The influence from the slight changes in the position d of the polarizer is also shown in Fig. 3(b). When d is varied within ±0.2 mm, the $|S_{11}|$ remains below -20 dB and the variation of peak gain is within ±0.15 dBi. This exhibits a good assembling tolerance. The comparison of radiation patterns for the proposed 2×2-subarray antennas with and without the polarizer along the planes of ϕ=45°and 135° is shown in Fig. 4. It should be noted that the linear polarization of the 2×2-subarray antenna shifts to the plane of ϕ=135° by using the 45° linear polarizer. So the planes of ϕ=135° and 45° become the intended E- and H-planes. Fig. 4 shows that the main beam and the first SLL with the polarizer in the intended E- and H-planes are nearly the same as the patterns without the polarizer except for some slight difference in the region of θ>35°. The cross-polarization level of the subarray with the polarizer is 8 dB higher than the one without the polarizer. Nonetheless, it is still suppressed by as much as 38.3 dB, representing a very good cross-polarization level. As a result, it is expected that the polarizer only shifts the linear polarization direction with little influence on antenna performance.

Due to the limitation to our computation power, we were not able to simulate the 32-slot array with the polarizer. However, the analysis and comparative study based on the smaller array provide us with a high confidence in the polarizer's ability to realize the 45° polarization change without affecting the radiation performance. Simulated radiation patterns of the 32-slot CTS array antenna (without polarizer) at the center frequency are shown in Fig. 5. The first SLLs in ϕ=90° and 0° are 26.3 dBi (corresponding to 13.4 dB suppression). They are reduced to 12.7 dBi (corresponding to an increased suppression

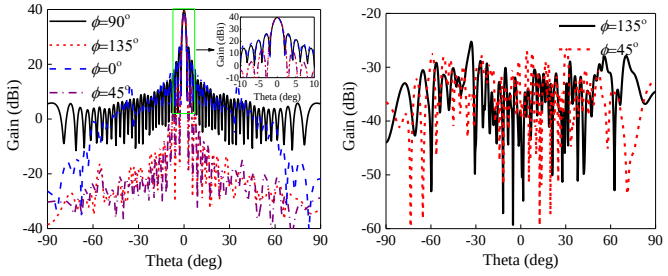

(a) (b)

Fig. 5 Simulated radiation patterns of the 32-slot CTS array in Fig. 1(a): (a) 2-D co-polarization patterns; (b) Cross-polarization patterns.

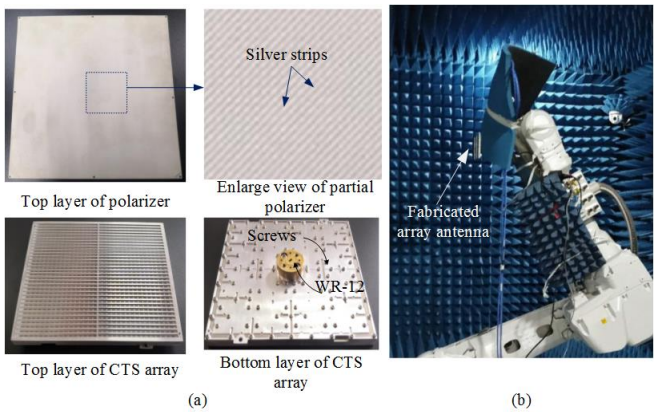

(a) (b)

Fig. 6 Photographs. (a) Fabricated polarizer and CTS array; (b) test environment.

of 27 dB) in the planes of ϕ=135° and 45°, as shown in Fig. 5(a). In addition, the radiation pattern masks in the planes of ϕ=135° and 45° are also much lower, which helps to satisfy the requirement by the ETSI or FCC. As discussed above, the linear polarization direction of the 32-slot CTS array has been shifted to ϕ=135° by using the polarizer, so that a low SLL and radiation pattern mask can be achieved. The cross-polarization patterns in the planes of ϕ=135° and 45° are shown in Fig. 5(b). The peaks of the cross-polarization patterns are lower than -25 dBi, which gives more than 65 dB suppression. Considering the addition of the polarizer would increase the cross-polarization level by 8 dB according to Fig. 4(b), the cross-polarization suppression of the whole array antenna including the polarizer is still over 57 dB, securing the low SLL and cross-polarization characteristics.

III. Experimental Results

The prototype is fabricated out of aluminum by milling with a nominal fabrication tolerance of about 20 um, and the polarizer is silver-plated on polycarbonate. Tightening screws are used around the antenna to suppress the potential leakage from the contacts between layers. The photographs of the fabricated array antenna, as well as the test environment are shown in Fig. 6. The overall size of the array antenna is 115 mm × 112 mm × 11 mm. The radiation performance is measured using a far-field antenna test system. As pointed out in Section II-C, we were not able to simulate the whole array antenna with the 45° polarizer. For this reason, the following comparison will be made between the fabricated whole array antenna and

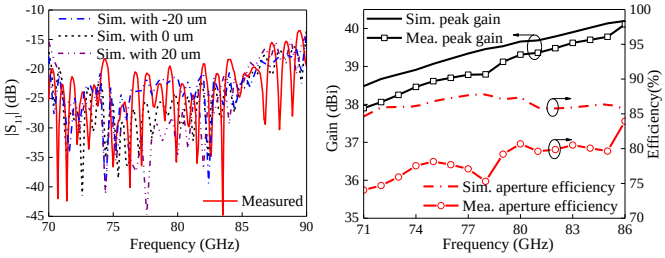

(a) (b)

Fig. 7 Simulated and measured results. (a) $|S_{11}|$; (b) Peak gain and aperture efficiency.

the simulated 32-slot CTS array without the polarizer).

Fig. 7(a) shows measured and simulated reflection coefficients. The measured reflection is higher than the simulated one. But it is still below -13 dB over the frequency range of 70-90 GHz. The small difference comes from two potential sources. One is the extra mismatch and assembling tolerance from the 45° linear polarizer as discussed around Fig. 3(b). The other is the fabrication tolerance. Its potential influence on the reflection coefficient has been investigated and estimated by changing the antenna parameters by ±20 μm, as shown in Fig. 7(a). This broadly confirms the contribution of fabrication tolerance to the difference.

Simulated and measured peak gains and aperture efficiency are shown in Fig. 7(b). The measurement shows an increasing peak gain response from 37.9 dBi to 40.1 dBi with frequency from 71 to 86 GHz. This only marginally missed the ETSI EN 302 standard (>38 dBi) at the lowest frequency by 0.1 dB [19]. A stable and high aperture efficiency of over 74% is achieved across the same frequency band. The measured gain is around 0.6 dB lower than the simulated one. The small difference is attributable to the fabrication and assembling tolerance, and the insertion loss (less than 0.3 dB from Fig. 3(b)) of the polarizer which was not included in the simulation.

Fig. 8 shows simulated and measured normalized radiation patterns in the intended E- and H-planes at different frequencies. A good agreement is obtained between the simulated and measured: the main lobes match perfectly and the measured sidelobe distribution are slightly higher. The small difference in the sidelobe distribution is mainly caused by the influence of the 45° linear polarizer as the simulation does not include the polarizer. The measurement uncertainty as well as the imperfection in fabrication and assembly are also factors. Over the entire E-band, the measured 3-dB beamwidths are less than 2° both in the intended and principal E- and H-planes. With the help of the linear polarizer, the measured SLLs in the intended E- and H-planes are suppressed by more than 25.5 dB and the whole radiation patterns are set to approach the ETSI class-IV envelope standard [19]. The measured cross-polarization levels are as low as −41 dB in the intended E- and H-planes. No simulation of the cross-polarization is included to avoid confusion as the polarizer would have a relatively large influence on the cross-polarization response as discussed around Fig. 4(b).

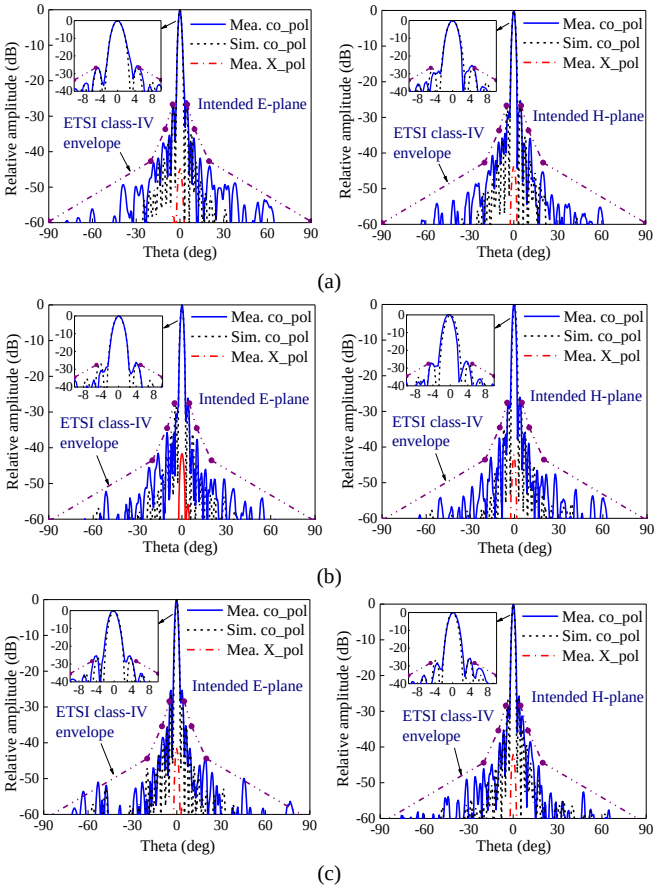

Fig. 8. Simulated and measured radiation patterns at (a) 71 GHz, (b) 78.5 GHz, (c) 86 GHz.

IV. Conclusion

In this letter we have proposed and demonstrated an E-band high aperture efficiency and low SLL 32-slot CTS array antenna using a 45° linear polarizer. 32 multiple-aperture excited PPWs have been employed to generate the quasi-TEM wave with a uniform amplitude distribution, so that a high aperture efficiency can be achieved. With the separated and optimally placed 45° linear polarizer, the antenna has realized a low SLL and cross-polarization, while maintaining its high aperture efficiency. Good agreement between the measurement of the prototype and simulation has been achieved.

References

[1] P. Liu, J. Liu, W. Hu, and X. Chen, "Hollow waveguide 32 × 32-slot array antenna covering 71–86 GHz band by the technology of a polyetherimide fabrication," *IEEE Antennas Wireless Propag. Lett*., vol. 17, no. 9, pp. 1635-1638, Sep. 2018.

[2] Y. Yu, W. Hong, Z. H. Jiang, and H. Zhang, "E-band low-profile, wideband 45° linearly polarized slot-loaded patch and its array for millimeter-wave communications," *IEEE Trans. Antennas Propag*., vol. 66, no. 8, pp. 4364–4369, Aug. 2018.

[3] A. Ghasemi and J. Laurin, "Beam steering in narrow-wall slotted ridge waveguide antenna using a rotating dielectric slab," *IEEE Antennas Wireless Propag. Lett*., vol. 17, no. 10, pp. 1773-1777, Oct. 2018.

[4] G. L. Huang, S. G. Zhou, T. H. hio, H. T. Hui, and T. S. Yeo, "A low profile and low sidelobe wideband slot antenna array feb by an amplitude-tapering waveguide feed-network" *IEEE Trans. Antennas Propag*., vol. 53, no. 1, pp. 419–423, Jan. 2015.

[5] W. W. Milroy, "The continuous transverse stub (CTS) array: basic theory, experiment, and application," in *Proc. Antenna Appl. Symp.*, 1991, pp. 253–283.

[6] X.-X. Yang, L. Di, Y. Yu, and S. Gao, "Low-profile frequency-scanned antenna based on substrate integrated waveguide," *IEEE Trans. Antennas Propag.*, vol. 65, no. 4, pp. 2051–2056, Apr. 2017.

[7] X. Lu, S. Gu, X. Wang, H. Liu, and W. Lu, "Beam-scanning continuous transverse stub antenna fed by a ridged waveguide slot array", *IEEE Antennas Wireless Propag. Lett*., vol. 16, pp. 1675–1678, Feb. 2017.

[8] F. F. Manzillo, M. Smierzchalski, L. L. Coq, M. Ettorre, J. Aurinsalo, K. T. Kautio, M. S. Lahti, A. E. I. Lamminen, J. Saily, and R. Sauleau, "A wide-angle scanning switched-beam antenna system in LTCC technology with high beam crossing levels for V-band communications", *IEEE Trans. Antennas Propag*., vol. 67, no. 1, pp. 541-553, Jan. 2019.

[9] Y. Lu, Q. You, Y. Wang, Y. You, J. Huang, and K. Wu, "Millimeter-wave low profile continuous transverse stub arrays with novel linear source generators", *IEEE Trans. Antennas Propag*., vol. 67, no. 2, pp. 988-997, Feb. 2019.

[10] T. Potelon, M. Ettorre, L. L. Coq, T. Bateman, J. Francey, D.Lelaidier, E. Seguenot, F. Devillers and R. Sauleau, "A low-profile broadband 32-slot continuous transverse stub array for backhaul applications in E-band," *IEEE Trans. Antennas Propag*., vol. 65, no. 12, pp. 6307–6316, Dec. 2017.

[11] T. Potelon, M. Ettorre and R. Sauleau, "Long slot array fed by a non-uniform corporate feed network in PPW technology," accepted by *IEEE Trans. Antennas Propag*., 2019. doi: 10.1109/TAP.2019.2917581

[12] J. Lin, W. Shen and K. Yang, "A low-sidelobe and wideband series-fed linear dielectric resonator antenna array," *IEEE Antennas Wireless Propag. Lett*., vol. 16, pp. 513-516, 2017.

[13] L. Shi, C. Bencivenni, R. Maaskant, J. Wettergren, J. Pragt and M. Ivashina, "High-efficiency and wideband aperiodic array of uniformly excited slotted waveguide antennas designed through compressive sensing," *IEEE Trans. Antennas Propag*., vol. 67, no. 5, pp. 2992-2999, May 2019.

[14] T. Tomura, Y. Miura, M. Zhang, J. Hirokawa, and M. Ando, "A 45° linearly polarized hollow-waveguide corporate-feed slot array antenna in the 60-GHz band," *IEEE Trans. Antennas Propag*., vol. 60, no. 8, pp. 3640–3646, Aug. 2012.

[15] T. Tomura, J. Hirokawa, T. Hirano, and M. Ando, "A 45° linearly polarized hollow-waveguide 16×16-slot array antenna covering 71–86 GHz band," *IEEE Trans. Antennas Propag*., vol. 62, no. 10, pp. 5061–5067, Oct. 2014.

[16] A. Vosoogh, P.-S. Kildal, and V. Vassilev, "Wideband and high-gain corporate-fed gap waveguide slot array antenna with ETSI Class II radiation pattern in V-Band," *IEEE Trans. Antennas Propag*., vol. 65, no. 4, pp. 1823–1831, Apr. 2017.

[17] Y. Miura, J. Hirokawa, T. Hirano, M. Ando, Y. Shibuya, and G. Yoshida, "Double-layer full-corporate-feed hollow-waveguide slot array antenna in the 60-GHz band," *IEEE Trans. Antennas Propag*., vol. 59, no. 8, pp. 2844–2851, Aug. 2011.

[18] R. P. Torres, and M. F. Chtedra, "Analysis and design of a two-octave polarization rotator for microwave frequency", *IEEE Trans. Antennas Propag*., vol. 41, no. 2, pp. 208–213, Feb. 1993.

[19] Fixed Radio Systems, Characteristics and requirements for point-to-point equipment and antennas, ETSI EN 302 217-4-2, v1. 5.1, (01-2010), 2010. Available: https://www.etsi.org/index.php